

# Stochastic many-body perturbation theory for electron correlation energies

Zhendong Li<sup>1, a)</sup>

Key Laboratory of Theoretical and Computational Photochemistry, Ministry of Education, College of Chemistry, Beijing Normal University, Beijing 100875, China

Treating electron correlation more accurately and efficiently is at the heart of the development of electronic structure methods. In the present work, we explore the use of stochastic approaches to evaluate high-order electron correlation energies, whose conventional computational scaling is unpleasantly steep, being  $O(N^{n+3})$  with respect to the system size  $N$  and the perturbation order  $n$  for the Møller-Plesset (MP) series. To this end, starting from Goldstone's time-dependent formulation of *ab initio* many-body perturbation theory (MBPT), we present a reformulation of MBPT, which naturally leads to a Monte Carlo scheme with  $O(nN^2 + n^2N + f(n))$  scaling at each step, where  $f(n)$  is a function of  $n$  depending on the specific numerical scheme. Proof-of-concept calculations demonstrate that the proposed quantum Monte Carlo algorithm successfully extends the previous Monte Carlo approaches for MP2 and MP3 to higher orders by overcoming the factorial scaling problem. For the first time the Goldstone's time-dependent formulation is made useful numerically for electron correlation energies, not only being purely as a theoretical tool.

## I. INTRODUCTION

The development of accurate and efficient methods for electron correlations is an enduring frontier in quantum chemistry. For weakly correlated systems, the many-body perturbation theory (MBPT) and the coupled-cluster (CC) theory<sup>1</sup> have been well-established as the standard tools due to their high accuracy and size extensivity. The latter property is essential for large systems. However, their unfavorable scalings make the application to situations that require high accuracy still being a significant challenge. Important situations include the studies of polymorphism of pharmaceutical solids<sup>2</sup> and relative stabilities of different structures of water clusters<sup>3</sup>, which typically require an accuracy of 0.1kcal/mol. Although local correlation methods<sup>4-6</sup> with reduced scalings have been significantly advanced in recent years, the lack of a method to benchmark their accuracies for large systems is also a problem to be solved. Due to its low scaling  $O(N^3)$  with  $N$  being the system size, the diffusion quantum Monte Carlo (DMC)<sup>7,8</sup> is gaining increasing popularity for large systems in recent years. However, the errors introduced by the fixed node approximation also require careful calibrations. Therefore, there is clearly still a need for developing methods with guaranteed accuracy for large systems even in the weakly correlated regime.

Motivated by various recent developments of quantum Monte Carlo (QMC) algorithms in *ab initio* quantum chemistry and condense matter physics<sup>9-30</sup>, in the present work, we explore the possibility of using stochastic approaches to evaluate high-order electron correla-

tion energies. Specifically, we will present a reformulation of standard MBPT into a general mathematical form, which is more suitable for Monte Carlo evaluations. In sharp contrast to the steep scaling  $O(N^{n+3})$  of the conventional algorithm<sup>31</sup> for the  $n$ -th order in the Møller-Plesset<sup>32</sup> (MP) series, the resulting QMC algorithm for evaluating the correlation energies scales as  $O(N^2)$  with respect to the system size. It deserves to be emphasized that although it is well-known that MBPT is less robust than CC and may fail to converge even for simple weakly correlated systems<sup>33</sup>, having the ability to compute high order MP $n$  energies for large systems is still highly valuable. Because mathematically the convergence issue can be overcome when more information about the behaviors of the MP series is available. This has been demonstrated for small molecules via resummation techniques<sup>34</sup>. In view of its low scaling, the proposed QMC algorithm may potentially open up the possibility to compute large systems (or small systems but with very large basis sets) with high accuracy without resorting to any local approximation.

## II. RECAPITULATION OF MBPT

To begin with, we briefly recapitulate the standard MBPT in Goldstone's time-dependent formulation<sup>35</sup>, which is the starting point of our reformulation of MP $n$  correlation energies. For simplicity, we will focus on the MP partition, viz.,  $\hat{H} = \hat{H}_0 + \hat{V}$  with  $\hat{H}_0 = \sum_p \varepsilon_p a_p^\dagger a_p$ , where the zeroth order state is the *canonical* Hartree-Fock (HF) reference  $|\Phi_0\rangle = |\Phi_{\text{HF}}\rangle$  and  $\hat{V} = \hat{V}_{ee} - \hat{V}_{\text{HF}}$ . The Goldstone's linked-cluster theorem<sup>35</sup> states that the  $(n+1)$ -th order correlation energy is given by

$$E_{n+1} = \lim_{\epsilon \rightarrow 0} \frac{(-i)^n}{n!} \int_{-\infty}^0 dt_1 \cdots dt_n e^{-\epsilon(|t_1| + \cdots + |t_n|)} \langle \Phi_0 | \hat{V}_I(0) T[\hat{V}_I(t_1) \cdots \hat{V}_I(t_n)] | \Phi_0 \rangle_c, \quad (1)$$

<sup>a)</sup>Electronic mail: zhendongli2008@gmail.com

where  $\hat{V}_I(t) = e^{i\hat{H}_0 t} \hat{V} e^{-i\hat{H}_0 t}$  is the corresponding perturbation operator in the interaction picture and the subscript 'c' indicates the connected parts. For the Coulomb interaction,  $\hat{V}_{ee}$  can be written as

$$\hat{V}_{ee} = \frac{1}{2} \int dx_1 dx'_1 v(x_1, x'_1) \hat{\psi}^\dagger(x_1) \hat{\psi}^\dagger(x'_1) \hat{\psi}(x'_1) \hat{\psi}(x_1) \quad (2)$$

where  $x_1 \triangleq (\sigma_1, \vec{r}_1)$  and  $x'_1 \triangleq (\sigma'_1, \vec{r}'_1)$  are composite indices for spin and spatial variables,  $v(x_1, x'_1) = \delta_{\sigma_1 \sigma'_1} / |\vec{r}_1 - \vec{r}'_1|$ , and the integration over  $x_1$  implies both a summations over spin  $\sigma_1 \in \{\alpha, \beta\}$  and an integration over spatial coordinates  $\vec{r}_1 \in \mathbb{R}^3$ . For brevity, we also introduce a compact notation  $\hat{\psi}^{(\dagger)}(1) \triangleq \hat{\psi}^{(\dagger)}(x_1, t_1)$  to represent operators in the interaction/Heisenberg picture by defining  $1 \triangleq (t_1, \sigma_1, \vec{r}_1)$ .

Since  $\hat{H}_0$  is quadratic, the (physical) vacuum expectation value in Eq. (1) can be evaluated using the Wick's theorem<sup>36</sup>, which implies a factorization of high-order noninteracting Green's functions into a sum over products of one-body Green's function (propagators)<sup>37</sup>,

$$\begin{aligned} & G^0(1, \dots, n; 1', \dots, n') \\ & \triangleq (-i)^n \langle \Phi_0 | T[\hat{\psi}(1) \dots \hat{\psi}(n) \hat{\psi}^\dagger(n') \dots \hat{\psi}^\dagger(1')] | \Phi_0 \rangle \\ & = \det(\mathbf{G}_n^0), \end{aligned} \quad (3)$$

where  $\mathbf{G}_n^0$  is an  $n$ -by- $n$  matrix with entries  $(\mathbf{G}_n^0)_{kl} \triangleq G^0(k, l) = -i \langle \Phi_0 | T[\hat{\psi}(k) \hat{\psi}^\dagger(l)] | \Phi_0 \rangle$ . Applying the Wick's theorem (3) in Eq. (1) and expanding the determinant, each product can be represented by a Feynman (Goldstone) diagram either connected or disconnected, and the linked cluster theorem<sup>35</sup> states that only the connected parts contribute to  $E_{n+1}$ . This is the standard way to derive Feynman diagrams in MBPT. However, for our purpose, we will keep Eq. (3) in its unexpanded form. The central result of this work is to

show that for the ground state (a more precise condition will be given in Sec. III), Eq. (1) can be recast into the following general mathematical form, which is more suitable for stochastic evaluations than the form based on Feynman (Goldstone) diagrams,

$$E_{n+1} = \frac{(-1)^n}{2^{n+1} n!} \int d\nu'_0 d\nu_1 \dots d\nu_n w_{n+1} \kappa_{n+1}. \quad (4)$$

The meaning of notations are explained as follows:  $w_{n+1} \triangleq v_0 v_1 \dots v_n$  with the interaction  $v_n \triangleq v(x_n, x'_n)$ ,  $\nu_n \triangleq (\tau_n, \sigma_n, \vec{r}_n, \sigma'_n, \vec{r}'_n)$  is a collection of all coordinates for the pair of electrons originated from the same  $\hat{V}_I(t_n)$ ,  $\tau_n$  is used to differentiate the imaginary time variable from the corresponding real time  $t_n$ , see Sec. III. The prime in  $\nu'_0$  (4) indicates that the integrations over  $\nu_0$  exclude the time integration, since  $\tau_0 = t_0 = 0$  from Eq. (1). The most important part  $\kappa_{n+1}$  in Eq. (4) is a function of all variables  $\kappa_{n+1}(\nu_0, \nu_1, \dots, \nu_{n+1})$  and will be discussed in Sec. IV.

### III. IMAGINARY-TIME FORMULA FOR ZERO-TEMPERATURE CORRELATION ENERGIES

To recast Eq. (1) into a form shown in Eq. (4), we proceed in two steps. First, we show that under certain conditions, Eq. (1) can be rewritten in a form similar to the grand potential  $\Omega$  in the grand canonical ensemble in finite-temperature MBPT<sup>38,39</sup> (however, the subtle difference is discussed in Appendix). The precise statement is provided by the following theorem.

**Theorem 1** (imaginary-time formula). *Assuming the HF reference  $|\Phi_0\rangle$  is the ground state of  $\hat{H}_0$ ,  $E_{n+1}$  in Eq. (1) can be alternatively expressed by an "imaginary-time" analog, viz.,*

$$E_{n+1} = \frac{(-1)^n}{n!} \int_{-\infty}^0 d\tau_1 \dots d\tau_n \langle \Phi_0 | \hat{V}_I(0) T[\hat{V}_I(\tau_1) \dots \hat{V}_I(\tau_n)] | \Phi_0 \rangle_c, \quad (5)$$

where  $\hat{V}_I(\tau) = e^{\tau(\hat{H} - \mu\hat{N})} \hat{V} e^{-\tau(\hat{H} - \mu\hat{N})}$  and the analog of "chemical potential"  $\mu$  is an arbitrary constant here.

The form (5) is more computational appealing, since it only involves real quantities, whereas Eq. (1) involves oscillating complex quantities arising from  $e^{i\hat{H}_0 t}$ , which will make the later stochastic evaluation more challenging in general. Besides, the unpleasant adiabatic factor  $e^{-\epsilon|t|}$  is also removed from Eq. (1).

There are several ways to derive Eq. (5), but the most obvious way is to consider the well-known time-independent expression<sup>35</sup> derived from Eq. (1),

$$E_{n+1} = (-1)^n \sum_{\{I_i\}} \left( V_{0I_1} \frac{1}{\omega_{I_1}} V_{I_1 I_2} \frac{1}{\omega_{I_2}} \dots \frac{1}{\omega_{I_n}} V_{I_n 0} \right)_c \quad (6)$$

where  $V_{I_1 I_2} = \langle \Phi_{I_1} | \hat{V} | \Phi_{I_2} \rangle$  with  $|\Phi_{I_i}\rangle$  being interme-

mediate states, and  $1/\omega_I \triangleq 1/(E_I - E_0)$  represents the energy denominator. By performing a Laplace transform  $1/\omega_I = \int_{-\infty}^0 d\tau e^{\omega_I \tau}$  and reversing the derivation from time-dependent PT (1) to time-independent PT (6), we can derive Eq. (5) from Eq. (6). However, two differences need to be noted.

First, the condition for the Laplace transform requires  $\omega_I > 0$  for all intermediate states, and hence Eq. (5) is valid only for the case that  $|\Phi_0\rangle$  is the ground state of  $\hat{H}_0$ , whereas Eq. (1) based on the Gell-Mann-Low theorem<sup>40</sup> in principle also works for excited states. Since we are mainly focused on the ground state problem in this work, this condition is usually satisfied.

Second, in Eq. (5) we have introduced a parameter  $\mu$ , which formally corresponds to the chemical potential in finite temperature MBPT. But here it is com-

pletely arbitrary, as can be seen in Eq. (6), because as long as  $\hat{V}$  does not change the particle number,  $\mu$  will be exactly cancelled in taking energy differences in the denominator  $1/\omega_I$ . However, for numerical convenience, we can choose it to be a value within the gap between the HOMO (highest occupied molecular orbital) and the LUMO (lowest unoccupied molecular orbital), e.g.,  $\mu = \frac{\varepsilon_{\text{HOMO}} + \varepsilon_{\text{LUMO}}}{2}$  used in the present work, such that given  $|\Phi_0\rangle$ , we have  $\varepsilon'_i \triangleq \varepsilon_i - \mu < 0$  for occupied orbitals and  $\varepsilon'_a \triangleq \varepsilon_a - \mu > 0$  for virtual orbitals. This will make the exponential factor in the following imaginary time Green's function  $G^0(k, l)$ , appearing in the counterpart of Eq. (3), always smaller than one,

$$\begin{aligned} G^0(k, l) &= \theta(\tau_{kl})G^0_{>}(k, l) + \theta(-\tau_{kl})G^0_{<}(k, l), \\ G^0_{>}(k, l) &= -\delta_{\sigma_k\sigma_l} \sum_a e^{-\varepsilon'_a\tau_{kl}} \psi_{a\sigma_k}(\vec{r}_k) \psi_{a\sigma_k}^*(\vec{r}_l), \\ G^0_{<}(k, l) &= \delta_{\sigma_k\sigma_l} \sum_i e^{-\varepsilon'_i\tau_{kl}} \psi_{i\sigma_k}(\vec{r}_k) \psi_{i\sigma_k}^*(\vec{r}_l), \end{aligned} \quad (7)$$

where  $\tau_{kl} \triangleq \tau_k - \tau_l$ . The same trick was previously introduced in the Laplace-transformed MP2<sup>41</sup>.

Alternatively, the above results can be derived from Eq. (1) by analyzing each *connected* Goldstone diagram and performing an analytic continuation of the real time integration to the imaginary time. We will not go into the details, but just mention that the same condition  $\omega_I > 0$  in this case will come from the requirement to guarantee that the contour integral over the arc goes to zero.

#### IV. SUMMATION OF DIAGRAMS BY MOMENT-CUMULANT RELATIONS

The next step is to express Eq. (5) into Eq. (4). Applying the imaginary-time analogy of the Wick's theorem (3) in Eq. (5), the expectation value  $\langle \Phi_0 | \hat{V}_I(0) T[\hat{V}_I(\tau_1) \cdots \hat{V}_I(\tau_n)] | \Phi_0 \rangle_c$  for  $E_{n+1}$  will become  $\frac{1}{2^n} w_{n+1} \det_c(\mathbf{G}_{2n+2}^0)$ , where again the subscript 'c' is used to denote the connected contributions. For small  $n$ ,  $\det_c(\mathbf{G}_{2n+2}^0)$  can be explicitly expanded, which corresponds to the use of Goldstone diagrams as employed in MC-MP2 (Monte Carlo MP2) and MC-MP3 by Hirata et al.<sup>14,15</sup>. However, this approach quickly becomes inefficient as  $n$  increases, since the number of diagrams increases *factorially*. While there are only 2 diagrams for MP2 and 12 diagrams for MP3, MP4 and MP5 have 300 and 13680 Goldstone diagrams<sup>42-44</sup>, respectively. Recently, in the context of diagrammatic Monte Carlo, which samples all Feynman diagrams stochastically, a trick to sum all connected diagrams at order  $n$  was proposed by Rossi<sup>29</sup>, by recursively subtracting disconnected contributions from determinants containing all diagrams. It has an exponential scaling  $O(2^n n^3 + 3^n)$ , but is less than factorial and has allowed to sum diagrams at order as high as 10 for the Hubbard model<sup>29</sup>. The same recursive formula (vide post) can be applied to compute  $\det_c(\mathbf{G}_{2n+2}^0)$  from  $\det(\mathbf{G}_{2n+2}^0)$  for correlation energies in Eq. (5). In the following context, we

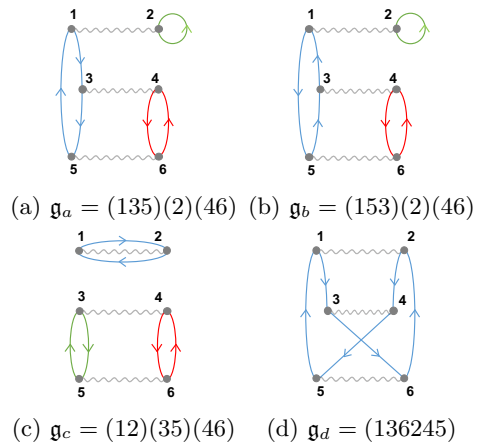


FIG. 1. Examples for cycle decomposition of permutations  $\mathbf{g} \in S_6$  and the loop structures of diagrams in MBPT. The loops formed by Green's functions highlighted by different colors are the basic building blocks, and they are glued together by interaction lines (wiggles) to form connected or disconnected diagrams.

provide a different derivation, which is more explicit and unveils the underlying fundamental moment-cumulant relation. More importantly, in this way we are able to write down an explicit expression for  $\det_c(\mathbf{G}_{2n+2}^0)$  in terms of principal minors of  $\det(\mathbf{G}_{2n+2}^0)$ .

#### 1. Loop expansion of determinants

To extract the connected part  $\det_c(\mathbf{G}_{2n+2}^0)$  from  $\det(\mathbf{G}_{2n+2}^0)$ , let us first consider the explicit formula for a determinant  $\det(\mathbf{A}_n)$  of an  $n$ -by- $n$  matrix  $\mathbf{A}_n$ ,

$$\det(\mathbf{A}_n) = \sum_{\mathbf{g} \in S_n} \text{sgn}(\mathbf{g}) A_{1,\mathbf{g}(1)} \cdots A_{n,\mathbf{g}(n)}, \quad (8)$$

where the summation is over all permutations  $\mathbf{g} (\in S_n)$  and  $\text{sgn}(\mathbf{g})$  is the signature of the permutation  $\mathbf{g}$ . For each permutation, we apply the cycle decomposition, e.g.,

$$\mathbf{g}_a = \begin{pmatrix} 1 & 2 & 3 & 4 & 5 & 6 \\ 3 & 2 & 5 & 6 & 3 & 4 \end{pmatrix} = (135)(2)(46). \quad (9)$$

Some typical examples are shown in Fig. 1 for  $n = 6$ . Since the signature  $\text{sgn}(\mathbf{g})$  can also be decomposed, e.g.,  $\text{sgn}(\mathbf{g}_a) = \text{sgn}((135))\text{sgn}((2))\text{sgn}((46)) = (-1)^{|(135)|-1}(-1)^{|(2)|-1}(-1)^{|(46)|-1}$ , where  $|{(135)}| = 3$  represents the length of the cycle (135), diagrammatically, we are able to rewrite each term in Eq. (8) as a product of *loops*, see Fig. 1. For example, the term for  $\mathbf{g}_a$  can be written compactly as  $l(135)l(2)l(46)$ , where the loop product  $l(i_1 i_2 \cdots i_k) \triangleq (-1)^{k-1} A_{i_1, i_2} \cdots A_{i_{k-1}, i_k} A_{i_k, i_1}$  for each cycle  $(i_1 i_2 \cdots i_k)$ . Then, the sum over  $n!$  permutations in Eq. (8) can be greatly simplified, by realizing that the sum over all the terms corresponding to the same set partition can be simplified into a single product, e.g.,  $(l(135) + l(153))l(2)l(46) \triangleq \kappa(\{1, 3, 5\})\kappa(\{2\})\kappa(\{4, 6\})$

for permutations  $\mathfrak{g}_a$  and  $\mathfrak{g}_b$  (see Fig. 1) generated from the set partition  $\pi = \{\{1, 3, 5\}, \{2\}, \{4, 6\}\}$ . Thus, through this construction, in general, we can express a determinant as a sum over partitions, where each partition contributes to a single product.

**Theorem 2** (loop expansion of determinants). *Given an elementary index set  $\mathcal{I} = \{1, \dots, n\}$ , Eq. (8) can be re-expressed as*

$$\det(\mathbf{A}_n) = \sum_{\pi} \prod_{I_k \in \pi} \kappa(I_k),$$

$$\kappa(I_k) = \sum_{i=1}^{(|I_k|-1)!} l_i(I_k). \quad (10)$$

where  $\pi$  represents a set partition of with length  $|\pi|$ , viz.,  $\pi = \{I_1, I_2, \dots, I_{|\pi|}\}$  with the  $k$ -th block  $I_k = \{i_1, i_2, \dots, i_{|I_k|}\}$ , and  $\kappa(I_k)$  is a sum over contributions from the  $(|I_k|-1)!$  possible cycles generated from the index set  $I_k$ , with  $l_i(I_k)$  being the loop contribution from one of the cycles.

In a Feynman (Goldstone) diagrammatic language, Eq. (10) is nothing but a mathematical description of the fact that loops formed by Green's functions are building block for all diagrams, as highlighted by different colors in Fig. 1 for selected third-order diagrams. Furthermore, the quantity  $\kappa(I_k)$  sums over all possible loops generated from the points in  $I_k$ . Therefore, if one-body operators are considered as the only perturbations, then  $\kappa(\mathcal{I})$  is simply the sum over all connected diagrams, because in this case the definition of connectivity with respect to perturbations coincides with the graphical definition. For two-body operators (2), the connectivity in  $\det_c(\mathbf{G}_{2n+2}^0)$ , defined with respect to the interaction lines (wiggles in Fig. 1), is different from that purely for Green's function lines. Fortunately, this complication can be treated by a generalized definition of  $\kappa$  in the next section.

## 2. Explicit expressions for $\kappa$ in Eq. (4)

For two-body perturbations, where different loops can be glued together by interaction lines to form a single connected diagrams, we can simple redefine the index set, viz.,  $\mathcal{I} = \{\nu_0, \dots, \nu_n\}$  for  $\det(\mathbf{G}_{2n+2}^0)$ , with each element corresponding to one interaction pair (i.e., two points in a graph). Then, it can be verified that exactly the same relation (10) also holds for this new index set  $\mathcal{I}$ . We illustrate this for the case  $\mathcal{I} = \{\nu_0, \nu_1\}$  with  $\nu_0 = \{1, 2\}$  and  $\nu_1 = \{3, 4\}$ . By defining generalized quantities  $\kappa(\{\nu_0\}) \equiv \kappa(\{\{1, 2\}\})$  and  $\kappa(\{\nu_0, \nu_1\}) \equiv$

$\kappa(\{\{1, 2\}, \{3, 4\}\})$  as

$$\begin{aligned} \kappa(\{\{1, 2\}\}) &\triangleq \kappa(\{1, 2\}) + \kappa(\{1\})\kappa(\{2\}), & (11) \\ \kappa(\{\{1, 2\}, \{3, 4\}\}) &\triangleq \kappa(\{1, 2, 3, 4\}) \\ &+ \kappa(\{1\})\kappa(\{2, 3, 4\}) + \kappa(\{2\})\kappa(\{1, 3, 4\}) \\ &+ \kappa(\{3\})\kappa(\{1, 3, 4\}) + \kappa(\{4\})\kappa(\{1, 2, 4\}) \\ &+ \kappa(\{1, 3\})\kappa(\{2, 4\}) + \kappa(\{1, 4\})\kappa(\{2, 3\}) \\ &+ \kappa(\{1, 3\})\kappa(\{2\})\kappa(\{4\}) \\ &+ \kappa(\{1, 4\})\kappa(\{2\})\kappa(\{3\}) \\ &+ \kappa(\{2, 4\})\kappa(\{1\})\kappa(\{3\}) \\ &+ \kappa(\{2, 3\})\kappa(\{1\})\kappa(\{4\}), & (12) \end{aligned}$$

where  $\kappa$  on the right hand sides are defined in Eq. (10) for the elementary index set  $\{1, 2, 3, 4\}$ , the determinant  $\det(\mathbf{A}_4)$  can be rewritten as  $\det(\mathbf{A}_4) = \kappa(\{\nu_0, \nu_1\}) + \kappa(\{\nu_0\})\kappa(\{\nu_1\})$ . It is of the same form as Eq. (10), but for partitions of  $\mathcal{I}$ , and  $\kappa(\{\nu_0, \nu_1\})$  now represents the target connected quantity  $\det_c(\mathbf{G}_{2n+2}^0)$ . The importance of the form (10) lies in that it is the same as the moment-cumulant relation in the multivariate case, such that the inversion of this relation is known. Summarizing these results, we have the following explicit expression for  $\det_c(\mathbf{G}_{2n+2}^0)$ .

**Theorem 3** (moment-cumulant relation). *Let  $\mathcal{I} = \{\nu_0, \dots, \nu_n\}$ , the moments defined as  $\mu(\mathcal{I}) \triangleq \det(\mathbf{G}_{2n+2}^0)$ , and other  $\mu(I_k)$  being the principal minors of  $\det(\mathbf{G}_{2n+2}^0)$  with both columns and rows constructed from  $I_k$ , the cumulant  $\kappa(\mathcal{I}) \triangleq \det_c(\mathbf{G}_{2n+2}^0)$  is given explicitly as*

$$\kappa(\mathcal{I}) = \sum_{\pi} (|\pi| - 1)! (-1)^{|\pi|-1} \prod_{I_k \in \pi} \mu(I_k), \quad (13)$$

which can be viewed as an inversion of the relation (10) in the particular setting.

It deserves to point out that the coefficient  $(|\pi|-1)!$  is nontrivial in the sense that it is a reflection of the non-trivial symmetric factors in diagrams for energy/free-energy, which are more complicated than those in diagrams for Green's functions (which would be simply one). The connection to the moment-cumulant relation is physically quite appealing, since it is a reflection of the linked cluster theorem<sup>35</sup>, and ensures that the correlation energy at each order is size-extensive.

## 3. Lowest order $\kappa^{\text{MP}n}$

The number of partitions in the sum (13) is given by the Bell number  $B_n$ , which are  $B_2 = 2$ ,  $B_3 = 5$ ,  $B_4 = 15$ , and  $B_5 = 52$  for the lowest few orders, and its growth, bound by  $(0.792n/\ln(n+1))^{n+1}$ <sup>45</sup>, is much slower than factorial. With the HF reference as in our case, Eq. (13) can be further simplified, since the effect of the term  $-\hat{V}_{\text{HF}}$  in  $\hat{V}$  is equivalent to set the diagonal 2-by-2 blocks of  $\mathbf{G}_{2n+2}^0$  be zero, such that  $\kappa(\{\nu_i\}) = \mu(\{\nu_i\}) = 0$ . Consequently, the lowest few orders can

be expressed compactly as

$$\kappa^{\text{MP2}} = \mu(\{\nu_0, \nu_1\}) \triangleq \mu_{01}, \quad (14)$$

$$\kappa^{\text{MP3}} = \mu(\{\nu_0, \nu_1, \nu_2\}) \triangleq \mu_{012}, \quad (15)$$

both of which just involve a single determinant. On the right hand sides, to make notations simpler, we have introduced a shorthand notation. Likewise,  $\kappa$  for MP4 and MP5 can be written compactly as

$$\kappa^{\text{MP4}} = \mu_{012} - \mu_{01}\mu_{23} - \mu_{02}\mu_{13} - \mu_{03}\mu_{12}, \quad (16)$$

$$\begin{aligned} \kappa^{\text{MP5}} = & \mu_{01234} \\ & - \mu_{012}\mu_{34} - \mu_{013}\mu_{24} - \mu_{014}\mu_{23} \\ & - \mu_{023}\mu_{14} - \mu_{024}\mu_{13} - \mu_{034}\mu_{12} \\ & - \mu_{01}\mu_{234} - \mu_{02}\mu_{134} - \mu_{03}\mu_{124} - \mu_{04}\mu_{123}. \end{aligned} \quad (17)$$

These expressions are remarkably simpler than the integrands based on the sum of individual Goldstone diagrams.

#### 4. Computational cost for evaluating $\kappa$

In general, the cost of Eq. (13) is  $O(2^n n^3)$  for computing all the moments  $\mu$  involved from principal minors of  $\mathbf{G}_{2n+2}^0$ , and  $O(nB_n)$  for assembling  $\kappa_{n+1}$  from Eq. (13), estimated by the number of multiplications. Thus, the use of the determinant trick to sum diagrams, which is a common technique in fermionic QMC for lattice models<sup>26,27</sup>, is essential to avoid the factorial complexity of diagrams at high orders. For  $n \geq 6$ , Eq. (13) starts to contain common intermediates shared by different set partitions, e.g.,  $-\mu_{0123}\mu_{45} + \mu_{01}\mu_{23}\mu_{45} = -(\mu_{0123} - \mu_{01}\mu_{23})\mu_{45}$ . Then, the recursive algorithm<sup>29</sup> becomes more advantageous. Having identified the moment-cumulant relation for  $\mu$  and  $\kappa$ , the recursive formula can be readily derived by translating the recursive relation<sup>46</sup> between multivariate moments and cumulants directly,

$$\kappa(\mathcal{I}) = \mu(\mathcal{I}) - \sum_{\mathcal{S} \subset \mathcal{I}', \mathcal{S} \neq \emptyset} \kappa(\{\nu_0\} \cup \mathcal{S}) \mu(\mathcal{I}' \setminus \mathcal{S}), \quad (18)$$

where  $\mathcal{I}' \triangleq \mathcal{I} \setminus \{\nu_0\}$ , and  $\mathcal{S} \neq \emptyset$  comes from the choice of HF reference. This can reduce the cost for assembling  $\kappa_{n+1}$  to  $O(3^n)$  asymptotically<sup>29</sup>.

#### V. MONTE CARLO ALGORITHM AND ILLUSTRATIVE EXAMPLE

After established the formula for MP $n$  correlation energies (4), we now consider its evaluations. The dimensionality of integrations for each  $\nu$  in Eq. (4) is 9 (including the sum over spins), and the total dimensionality is  $9n-1$  at order  $n$ , which makes Monte Carlo algorithms a natural choice. Specifically, at order  $n+1$ , we define an importance sampling function  $p_{n+1}(\nu_0, \dots, \nu_n) = \prod_{k=0}^n p(\nu_k)$  for the configuration

$$\mathcal{C}_{n+1} = \{\nu_0, \dots, \nu_n\},$$

$$p(\nu_k) = p(\tau_k)p(\sigma_k)p(\sigma'_k)p(\vec{r}_k, \vec{r}'_k),$$

$$p(\tau_k) = \Delta e^{\Delta\tau}, \quad \tau \in (-\infty, 0],$$

$$p(\sigma_k) = \frac{1}{2}, \quad \sigma \in \{\alpha, \beta\}, \quad (19)$$

where  $\Delta = \varepsilon_{\text{LUMO}} - \varepsilon_{\text{HOMO}}$  is the zeroth-order HF gap of the system. In this work, we investigated two choices for  $p(\vec{r}_k, \vec{r}'_k)$ ,

$$p_A(\vec{r}_k, \vec{r}'_k) = p(\vec{r}_k)p(\vec{r}'_k), \quad (20)$$

$$p_B(\vec{r}_k, \vec{r}'_k) = \frac{1}{E_J |\vec{r}_k - \vec{r}'_k|} p(\vec{r}_k)p(\vec{r}'_k), \quad (21)$$

where  $p(\vec{r}) = \frac{1}{K} \sum_{r=1}^K |\psi_r(\vec{r})|^2$ ,  $K$  is the dimensionality of molecular orbitals (MO), and  $E_J$  is a normalization factor. Note that for  $\nu_0$ , there is no need to generate  $\tau_0$ . The two electrons within the same pair are generated via the standard Markov Chain Monte Carlo (MCMC) method. Eq. (4) is then evaluated simply from the average  $\frac{(-1)^n}{2^{n+1}n!} \left\langle \frac{w_{n+1}\kappa_{n+1}}{p_{n+1}} \right\rangle_{p_{n+1}}$ . The entire algorithm is summarized in Fig. 2.

The expensive steps in each Monte Carlo step include:  $O(nK)$  for evaluating the values of atomic orbitals (AO) at the sampled spatial points and  $O(nK^2)$  for transformation from AO to MO in step 2 (line 7 in Fig. 2),  $O(n^2K)$  for constructing  $\mathbf{G}_{2n+2}^0$  in step 3 (line 10), and  $O(f(n))$  for evaluating  $\kappa_{n+1}$  in step 4 (line 11), where  $f(n)$  is a function depending on a specific numerical scheme (Eq. (13) or (18)) for  $\kappa_{n+1}$ . Thus, the total computational cost scales as  $O(nK^2 + n^2K + f(n))$ . For large systems, assuming  $K$  is proportional to the system size  $N$ , the present algorithm scales as  $O(N^2)$  asymptotically.

To examine the correctness of our formulation in the above sections, we have implemented the above algorithm in Fig. 2 in an in-house program package SMBPT, and studied the prototypical molecule  $\text{H}_2$  with STO-3G at the equilibrium geometry  $R_{\text{H-H}} = R_e = 0.74144\text{\AA}$  and a stretched geometry  $R_{\text{H-H}}=4\text{\AA}$  with Eqs. (20) (scheme A) and (21) (scheme B). Albeit being trivial for traditional quantum chemistry methods, this problem is nontrivial and considerably more complicated than the corresponding two-site Hubbard model for QMC due to the use of a realistic Coulomb interaction in real space. The data obtained with sample size being  $10^9$  are shown in Table I. Overall, we found the MP $n$  series can be reproduced by the present stochastic scheme at both geometries. Using the summation based on moment-cumulant relations, it successfully extends the previous MC methods<sup>14,15</sup> for MP2 and MP3 to higher orders with a reasonable computational cost. It can be seen that the scheme B leads to slightly more accurate results than the scheme A.

At higher orders, a new difficulty is found in stochastic evaluations of the MP $n$  series, which is not obvious in the study of low orders. From Table I, we observed a rapid growth of variance as  $n$  increases, in particular at the stretched geometry, where the interaction becomes stronger. This is likely due to both the simplicity of our

```

1: function SMBPT( $n$ )
2:   Randomly initialize a set of spatial coordinates  $\{(\vec{r}_k, \vec{r}'_k)\}_{k=0}^n$ 
3:   Compute values of molecular orbitals  $\{\psi_s(\vec{r})\}_{s=1}^K$  at  $\{(\vec{r}_k, \vec{r}'_k)\}_{k=0}^n$   $\triangleright O(nK^2)$ 
4:   loop
5:     Move  $\{(\vec{r}_k, \vec{r}'_k)\}_{k=0}^n$  randomly to new positions
6:     Update values of molecular orbitals  $\{\psi_s(\vec{r})\}_{s=1}^K$ 
7:     Metropolis update for spatial coordinates according to  $p(\vec{r}, \vec{r}')$  in Eq. (20) or (21)  $\triangleright O(nK^2)$ 
8:     if equilibrated then
9:       Generate imaginary times and spins according to Eq. (19) to form a configuration  $\mathcal{C}_{n+1}$ 
10:      Construct  $\mathbf{G}_{2n+2}^0$  for the given  $\mathcal{C}_{n+1}$  from  $\{\psi_s(\vec{r})\}_{s=1}^K$  and  $\{\varepsilon_s\}_{s=1}^K$  using Eq. (7)  $\triangleright O(n^2K)$ 
11:      Evaluate  $\kappa_{k+1}$  ( $1 \leq k \leq n$ ) from all principal minors  $\mu$  of  $\mathbf{G}_{2n+2}^0$  using Eq. (13) or (18)  $\triangleright O(f(n))$ 
12:      Compute  $\frac{w_{k+1}\kappa_{k+1}}{p_{k+1}}$  and estimates of  $E_{k+1}$  for all  $1 \leq k \leq n$ 
13:     end if
14:   end loop
15: end function

```

FIG. 2. Stochastic MBPT algorithm for correlation energies

TABLE I. Computed MP $n$  energies  $E_n$  for H<sub>2</sub> with STO-3G at the equilibrium geometry  $R_{\text{H-H}} = R_e$  and a stretched geometry  $R_{\text{H-H}}=4\text{\AA}$  using two different importance sampling functions (scheme A with (20) and scheme B with (21)). The sample size is  $N_{\text{MC}} = 10^9$ .

$n$	exact	scheme A (20)	scheme B (21)
$R_{\text{H-H}} = R_e$			
1	-0.67448	-0.67446±0.00005	-0.67450±0.00004
2	-0.01317	-0.01317±0.00001	-0.01317±0.00001
3	-0.00485	-0.00485±0.00000	-0.00485±0.00000
4	-0.00172	-0.00172±0.00000	-0.00172±0.00000
5	-0.00058	-0.00054±0.00003	-0.00059±0.00001
6	-0.00019	-0.00004±0.00012	-0.00022±0.00008
$R_{\text{H-H}}=4\text{\AA}$			
1	-0.45281	-0.45345±0.00073	-0.45282±0.00001
2	-0.38156	-0.38212±0.00133	-0.38210±0.00108
3	-0.37346	-0.37410±0.00120	-0.37353±0.00125
4	0.17304	0.17374±0.00370	0.17527±0.00360
5	1.22364	1.22205±0.00882	1.23131±0.00828
6	1.22515	1.15467±0.06289	1.23063±0.03087

importance sampling functions as well as the fermionic sign problem, since  $\kappa$  is not always positive. Therefore, while the obtained data are overall quite encouraging, further investigations are necessary to fully understand the exact origin of such problem. Along with other possible improvements, e.g., faster algorithms for computing  $\mu$  and assembling  $\kappa$ , alternative definitions for  $\kappa$ , as well as improved sampling techniques, this will be the subject of a subsequent study.

## VI. SUMMARY

In summary, we presented a reformulation of standard MBPT for correlation energies into a general form (4) using Theorems 1 and 3, which involves multidimensional integrations that can be evaluated by Monte Carlo algorithms. The proposed QMC algorithm share similarities with MC-MP2 and MC-MP3<sup>14,15</sup>, such as its low formal scaling  $O(N^2)$ , which makes it promising for large systems. The major differences are twofold. First, we use an efficient algorithm based on moment-

cumulant relations, which avoids the factorial scaling in using Goldstone diagrams. Second, in our algorithm all the spatial, spin, and imaginary time variables are sampled stochastically, which are necessary ingredients for high-order perturbation theories. Like FCIQMC<sup>10</sup> (full configuration interaction quantum Monte Carlo) and AFQMC<sup>25</sup> (auxiliary field QMC), the present QMC algorithm is formulated within an orbital space, but its evaluation in real space is more similar to standard VMC (variational MC) and DMC. The advantage of the real-space evaluation is its lower computational scaling and lower requirement for storage with respect to the system size. However, if full molecular integrals are affordable, as for small systems, it is also possible to adapt the present QMC algorithm to the sampling based on molecular integrals as in FCIQMC. Apart from correlation energies, several other extensions can be readily envisaged, such as the extension to the finite temperature case and physical properties other than energies. From a practical aspect, there are still a few obstacles to be overcome in future. Most importantly, improved sampling methods, along with ways to alleviate the fermionic sign problem, need to be developed in order to apply the stochastic MBPT to large basis sets and systems. Investigations along these lines are being carried out in our laboratory.

## ACKNOWLEDGEMENTS

Z.L. would like to thank Yunfeng Xiong and Dr. Sihong Shao (Peking University) for helpful discussions and the Beijing Normal University Startup Package.

## APPENDIX: DIFFERENCE BETWEEN EQ. (5) AND SIMILAR QUANTITIES IN FINITE-TEMPERATURE MBPT

We emphasize that while the expression of  $E_{n+1}$  in Eq. (5) is in a form similar to that in finite-temperature MBPT (FT-MBPT), this new formula for correlation energy at a given order does not correspond to any

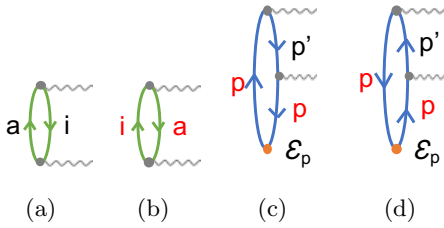


FIG. 3. Diagrams for one-body perturbation at the second order in FT-MBPT.

term in FT-MBPT in the zero-temperature limit. This reflects the general fact that zero-temperature MBPT (ZT-MBPT) is not the same theory as FT-MBPT in the zero-temperature limit<sup>47</sup>. Here, we illustrate the subtle differences between Eq. (5) and similar quantities in FT-MBPT in details. The most distinctive difference is that  $\mu$  in Eq. (5) can take arbitrary values, while in FT-MBPT it has a physical meaning and controls the average particle number. However, even if we assume the same  $\mu$  is used in Eq. (5) and FT-MBPT, Eq. (5) cannot be derived from FT-MBPT. For simplicity, we will just discuss the differences for gapped systems.

On the one hand, the corresponding quantity for grand potential  $\Omega_{n+1}$  of a similar form as Eq. (5) in FT-MBPT reads

$$\Omega_{n+1} = \frac{(-1)^n}{(n+1)!} \int_0^\beta d\tau_1 \cdots d\tau_n \langle T_\tau [\hat{V}_I(\tau_1) \cdots \hat{V}_I(\tau_n)] \hat{\mathcal{V}}_c \rangle$$

where the factor  $1/(n+1)!$  is different from that in Eq. (5). This nontrivial smaller factor precisely cancels the additional contributions from the ensemble average  $\langle \cdots \rangle$ , such that the value of  $\Omega_{n+1}$  goes to  $E_{n+1}$  in the zero-temperature limit, i.e.,  $\beta \rightarrow \infty$ . This can be illustrated by considering a one-body perturbation at the second order, see Fig. 3. In ZT-MBPT, only Fig. 3(a) contributes to  $E_2$ , while in FT-MBPT, the additional term Fig. 3(b) also survives for  $\Omega_2$  and has the same value as Fig. 3(a). Only by multiplying the factor  $1/2!$ ,  $\Omega_2$  will become the same as  $E_2$  in the zero-temperature limit.

On the other hand, the second order internal energy  $U_2$  in FT-MBPT contains two parts,

$$U_2 = \frac{(-1)^1}{1!} \int_0^\beta d\tau_1 \langle \hat{V}_I(\tau_1) \hat{V}_c \rangle + \frac{(-1)^2}{2!} \int_0^\beta d\tau_1 \int_0^\beta d\tau_2 \langle T_\tau [\hat{V}_I(\tau_1) \hat{V}_I(\tau_2)] \hat{H}_0 \rangle$$

The first part is similar to  $E_2$  in Eq. (5), except for the ensemble average. Thus, it will be twice of  $E_2$  as  $\beta \rightarrow \infty$ , due to the inclusion of both Figs. 3(a) and (b). Only when the two 'anomalous' diagrams (in the sense that the orbital index  $p$  appears both as particles and holes) from the second part of Eq. (23) are included, see Figs. 3(c) and (d), the additional contribution in the first part will be cancelled, such that  $U_2$  goes to the same value as  $E_2$  in the zero-temperature limit.

In sum, the formula for  $E_{n+1}$  (5) are different from those for  $\Omega_{n+1}$  and  $U_{n+1}$  in FT-MBPT, even though

their values will be the same in the zero-temperature limit given the same  $\mu$ . This novel formula for correlation energies, as a result of ZT-MBPT followed by a Laplace transformation to introduce an artificial imaginary time, cannot be obtained from any physical quantity in FT-MBPT by taking in the zero-temperature limit.

<sup>1</sup>I. Shavitt and R. J. Bartlett, *Many-body methods in chemistry and physics: MBPT and coupled-cluster theory* (Cambridge university press, 2009).

<sup>2</sup>G. J. Beran, *Chemical reviews* **116**, 5567 (2016).

<sup>3</sup>R. Ludwig, *Angewandte Chemie International Edition* **40**, 1808 (2001).

<sup>4</sup>S. Saebo and P. Pulay, *Annual Review of Physical Chemistry* **44**, 213 (1993).

<sup>5</sup>M. Schütz, G. Hetzer, and H.-J. Werner, *The Journal of chemical physics* **111**, 5691 (1999).

<sup>6</sup>C. Riplinger and F. Neese, *The Journal of chemical physics* **138**, 034106 (2013).

<sup>7</sup>W. Foulkes, L. Mitos, R. Needs, and G. Rajagopal, *Reviews of Modern Physics* **73**, 33 (2001).

<sup>8</sup>M. Dubecký, L. Mitos, and P. Jurečka, *Chemical reviews* **116**, 5188 (2016).

<sup>9</sup>A. J. Thom and A. Alavi, *Physical review letters* **99**, 143001 (2007).

<sup>10</sup>G. H. Booth, A. J. Thom, and A. Alavi, *The Journal of chemical physics* **131**, 054106 (2009).

<sup>11</sup>D. Cleland, G. H. Booth, and A. Alavi, *The Journal of chemical physics* **132**, 041103 (2010).

<sup>12</sup>A. J. Thom, *Physical review letters* **105**, 263004 (2010).

<sup>13</sup>C. J. Scott, R. Di Remigio, T. D. Crawford, and A. J. Thom, *The Journal of physical chemistry letters* **10**, 925 (2019).

<sup>14</sup>S. Y. Willow, K. S. Kim, and S. Hirata, *The Journal of chemical physics* **137**, 204122 (2012).

<sup>15</sup>S. Y. Willow and S. Hirata, *The Journal of chemical physics* **140**, 024111 (2014).

<sup>16</sup>S. Y. Willow, K. S. Kim, and S. Hirata, *The Journal of chemical physics* **138**, 164111 (2013).

<sup>17</sup>D. Neuhauser, E. Rabani, and R. Baer, *Journal of chemical theory and computation* **9**, 24 (2012).

<sup>18</sup>D. Neuhauser, Y. Gao, C. Arntsen, C. Karshenas, E. Rabani, and R. Baer, *Physical review letters* **113**, 076402 (2014).

<sup>19</sup>Y. Cytter, D. Neuhauser, and R. Baer, *Journal of chemical theory and computation* **10**, 4317 (2014).

<sup>20</sup>D. Neuhauser, R. Baer, and D. Zgid, *Journal of chemical theory and computation* **13**, 5396 (2017).

<sup>21</sup>W. Dou, T. Y. Takeshita, M. Chen, R. Baer, D. Neuhauser, and E. Rabani, *Journal of chemical theory and computation* (2019).

<sup>22</sup>S. Sharma, A. A. Holmes, G. Jeanmairet, A. Alavi, and C. J. Umrigar, *Journal of chemical theory and computation* **13**, 1595 (2017).

<sup>23</sup>Y. Garniron, A. Scemama, P.-F. Loos, and M. Caffarel, *The Journal of chemical physics* **147**, 034101 (2017).

<sup>24</sup>S. Guo, Z. Li, and G. K.-L. Chan, *The Journal of chemical physics* **148**, 221104 (2018).

<sup>25</sup>M. Motta and S. Zhang, *Wiley Interdisciplinary Reviews: Computational Molecular Science* **8**, e1364 (2018).

<sup>26</sup>A. Rubtsov and A. Lichtenstein, *Journal of Experimental and Theoretical Physics Letters* **80**, 61 (2004).

<sup>27</sup>A. N. Rubtsov, V. V. Savkin, and A. I. Lichtenstein, *Physical Review B* **72**, 035122 (2005).

<sup>28</sup>E. Gull, A. J. Millis, A. I. Lichtenstein, A. N. Rubtsov, M. Troyer, and P. Werner, *Reviews of modern physics* **83**, 349 (2011).

<sup>29</sup>R. Rossi, *Physical review letters* **119**, 045701 (2017).

<sup>30</sup>K. Van Houcke, I. S. Tupitsyn, and N. V. Prokofev, *Handbook of Materials Modeling: Methods: Theory and Modeling*, 1 (2018).

<sup>31</sup>D. Cremer, *Wiley Interdisciplinary Reviews: Computational Molecular Science* **1**, 509 (2011).

- <sup>32</sup>C. Møller and M. S. Plesset, *Physical review* **46**, 618 (1934).
- <sup>33</sup>J. Olsen, O. Christiansen, H. Koch, and P. Jørgensen, *The Journal of chemical physics* **105**, 5082 (1996).
- <sup>34</sup>D. Z. Goodson, *Wiley Interdisciplinary Reviews: Computational Molecular Science* **2**, 743 (2012).
- <sup>35</sup>J. Goldstone, *Proceedings of the Royal Society of London. Series A. Mathematical and Physical Sciences* **239**, 267 (1957).
- <sup>36</sup>G.-C. Wick, *Physical review* **80**, 268 (1950).
- <sup>37</sup>G. Stefanucci and R. Van Leeuwen, *Nonequilibrium many-body theory of quantum systems: a modern introduction* (Cambridge University Press, 2013).
- <sup>38</sup>C. Bloch and C. De Dominicis, *Nuclear Physics* **7**, 459 (1958).
- <sup>39</sup>A. L. Fetter and J. D. Walecka, *Quantum theory of many-particle systems* (McGraw-Hill: New York, 1971).
- <sup>40</sup>M. Gell-Mann and F. Low, *Physical Review* **84**, 350 (1951).
- <sup>41</sup>M. Häser and J. Almlöf, *The Journal of chemical physics* **96**, 489 (1992).
- <sup>42</sup>P. Rosky and M. Karplus, *The Journal of Chemical Physics* **64**, 1596 (1976).
- <sup>43</sup>S. Wilson, *Computer Physics Reports* **2**, 391 (1985).
- <sup>44</sup>S. A. Kucharski and R. J. Bartlett, in *Advances in quantum chemistry*, Vol. 18 (Elsevier, 1986) pp. 281–344.
- <sup>45</sup>D. Berend and T. Tassa, *Probability and Mathematical Statistics* **30**, 185 (2010).
- <sup>46</sup>P. J. Smith, *The American Statistician* **49**, 217 (1995).
- <sup>47</sup>W. Kohn and J. Luttinger, *Physical Review* **118**, 41 (1960).